



# Using local PHS+poly approximations for Laplace Transform Inversion by Gaver-Stehfest algorithm

Rosanna Campagna<sup>\*,a</sup> · Víctor Bayona<sup>b</sup> · Salvatore Cuomo<sup>c</sup>

Communicated by A. De Rossi

## Abstract

The Laplace transform inversion is a well-known ill-conditioned problem and many numerical schemes in literature have investigated how to solve it. In this paper, we revise the Gaver-Stehfest method by using polyharmonic splines augmented with polynomials to approximate the Laplace transform into the numerical inversion formula. Theoretical accuracy bounds for the fitting model are given. Discussions on the effectiveness of the inversion algorithm are produced and confirmed by numerical experiments about approximation errors and inversion results. Comparisons with an existing model are also presented.

## 1 Introduction

Suppose  $f$  is a real- or complex-valued function of the variable  $t > 0$  and  $z$  is a real or complex parameter. We define  $F(z)$  the Laplace transform of  $f$  as

$$F(z) = \int_0^{\infty} e^{-zt} f(t) dt = \lim_{\tau \rightarrow \infty} \int_0^{\tau} e^{-zt} f(t) dt, \quad (1)$$

whenever the limit exists (as a finite number). More in detail, a function  $f$  admits a Laplace transform if (a) it is almost everywhere defined in  $\mathbb{R}^+$ , measurable there with respect to the Lebesgue measure; (b) it is a locally integrable function in  $\mathbb{R}^+$ ; (c) there is at least one value  $z_0$  of the complex variable  $z$  for which the improper integral (1) converges. In this case, that integral is called the Laplace transform (Lt) of  $f$  at the point  $z_0$ . We focus on the design of a numerical method to compute  $f(t)$ , for any  $t \in (0, +\infty)$ , under the hypothesis that  $F$  is only evaluable on the real axis. This problem is generally known as *real inversion* of the Lt, whose ill-positioning imposes regularization techniques to deal with the strong ill-conditioning emerging in the numerical inversion methods. A wide literature concerns the Laplace inversion problem and it is mainly focused on: i) numerical methods; ii) algorithms and software; iii) the numerical stability of the computational procedures. The numerical inversion schemes are classified into several classes, more in detail methods compute a samples of  $f$  as the Gaver reported in [1, 2], methods which expand  $f$  in exponential functions reported by Doetsch in [3], methods based on Gaussian quadrature designed by Piessens [4], methods based on a bilinear transformation with a Laguerre expansion [5, 6], and finally, methods based on Fourier series as the Talbot formulas [7, 8]. Several of these schemes have been implemented in a mathematical software as, for examples, those based on discretization of the functional integral [9, 10, 11], or consisting in collocation methods [12]. About the stability of the numerical algorithms theoretical and computable estimates of the propagated errors in inversion formulas are reported in [13, 14]. More in general, we observe that all inversion formulas need an analytic form of the Laplace Transform  $F$  and  $F$  is evaluated in a finite number of points. Unfortunately, in many applications, the Lts are power-law, exponential, hyperbolic, logarithmic, trigonometric functions, but they are also expressed by the so-called *special functions*, i.e. the Error, Gamma and Bessel functions:

$$\operatorname{erf}(x) := \frac{1}{\sqrt{\pi}} \int_{-x}^x e^{-t^2} dt, \quad \Gamma(x) := \int_0^{\infty} t^{x-1} e^{-t} dt, \quad J_{-\nu}(x) := \sum_{n=0}^{\infty} \frac{(-1)^n}{n! \cdot \Gamma(n+1-\nu)} \left(\frac{x}{2}\right)^{2n-\nu}$$

so only a tabulated form for the Lt may be available, through numerical integration. According this, the known inversion formulas can *not* be applied, except by introducing a preprocessing stage consisting in a continuous functional approximation of  $F$  from a finite set of its values [15]. Here we focus on the Gaver-Stehfest inversion method (GS), defined in [16]. This scheme is used in several science and engineering applications. In [17], for example, the use of Laplace function in the solution of boundary value problems in applied mechanics is discussed, related to transient responses of isotropic and transversely isotropic half-space to concentrated impulse or those related to viscoelastic wave motion in layered media. In this work several methods are tested in

<sup>\*,a</sup>Corresponding author, Department of Mathematics and Physics, University of Campania “L. Vanvitelli”, Italy, rosanna.campagna@unicampania.it

<sup>b</sup>Departamento de Matemáticas, Universidad Carlos III de Madrid, Leganés, Spain, vbayona@math.uc3m.es

<sup>c</sup>Department of Mathematics and Applications, University of Naples Federico II, Italy, salvatore.cuomo@unina.it

problems such as those in boundary element or boundary integral equations, theoretical seismology, soil-structure-interaction in time domain. With respect of GS method, any value of the inverse function  $f(t)$  is obtained as a truncated sum of  $M$  weighted Lt evaluations at uniformly distributed points  $g_i = i \cdot \ln(2)/t$ ,  $i = 1, 2, \dots, M$ , named GS points (GSp). GS computes the approximation,  $f_F$ , of  $f(t)$  as:

$$f_F(t) = \frac{\ln(2)}{t} \sum_{i=1}^M V_i F(g_i), \quad (2)$$

with the coefficients  $V_i$  defined as (see [16] for more details)

$$V_i = (-1)^{i+M/2} \sum_{k=\lfloor(i+1)/2\rfloor}^{\min(i, M/2)} \frac{k^{M/2}(2k)!}{(M/2 - k)!k!(k-1)!(i-k)!(2k-i)!}, \quad (3)$$

which grow fast with the growth of  $M$ . Parameter  $M$ , referred to as the *Stehfest number*, should be even. The weighting coefficients  $V_i$  can be calculated once and for all during a pre-processing, because they only depend on the Stehfest number. The precision of the Gaver-Stehfest inversion method strongly depends on the Stehfest number  $M$  and multi-precision computing is suggested to improve the accuracy of such algorithm [18]. Truncating the expansion by considering  $M$  terms, defines an approximation inverse Lt,  $f_F$ , and introduces a *discretization error*:

$$\varepsilon_{discr}(t) := |f(t) - f_F(t)|, \quad (4)$$

depending on  $M$ , for any  $t \in (0, +\infty)$ . In this paper we propose a revision of the GS formula in (2), in which a fitting model approximating  $F$  is introduced, in order to face with the absence of useful information, when  $F$  is available only in discrete form. The fitting model is based on a combination of polyharmonic radial basis functions augmented with polynomials (PHS+poly) [19]. For a general discussion on Radial Basis Functions (RBFs) methods see [20], and for more details into this PHS+poly formulation see [21, 22, 23]. In particular, the reader is referred to [21] for an insight into the properties of RBF interpolation augmented with polynomials. In the following section, two theorems will be given concerning, respectively, the order of accuracy inside and outside the knots interval. Starting from an estimate for the order of convergence between the knots [21], we define a similar result *out of samples*. In the context of the Laplace transform inversion, the *extrapolation* of information from data, outside the samples domain, is a crucial point in order to makes inversion reliable. The interpolating model could fail or introduce a too high fitting error with respect to its amplification due to the conditioning of the inversion formula, so making the inversion unreliable. We highlight that the reliability of the inversion formula strongly depends on several parameters, as for example, in GS, the number  $M$  of terms, the accuracy in computation of the  $V_i$  weights and the approximation of the Lt  $F$ . The main contribution of this paper is to provide theoretical accuracy bounds for the fitting model and discussions on the effectiveness of the related inversion algorithm.

The paper is organized as follows. In section 2 we present the PHS+poly model and give theoretical estimates on the local and asymptotic accuracy. In section 3 some a priori error bounds allow controlling the error propagation due to the Lt approximation, on the computed inverse solution. In section 4, we give numerical results on the error estimates of the revised method and comparisons with a published method. The last section refers final conclusions.

## 2 Local PHS+poly approximations

Local RBF approximations based on infinitely smooth RBFs, such as Multiquadrics (MQ)  $\phi(r) = \sqrt{1 + \varepsilon^2 r^2}$  or Gaussians (GA)  $\phi(r) = e^{-\varepsilon^2 r^2}$ , have been extensively used in the past decades (see [24] for an overview). This approach, which feature a shape parameter  $\varepsilon$ , can lead to very accurate approximations in the near flat-limit  $\varepsilon \rightarrow 0$ . However, this limit is numerically ill-conditioned and cannot be achieved by direct methods. Several methods (e.g. RBF-GA, RBF-QR and RBF-RA) have been developed to compute this limit accurately (see [24] for a detailed description).

Recently, it has been found that the combination of polyharmonic splines (PHS),  $\phi(r) = r^{2m-1}$ ,  $r \in \mathbb{R}^+$ ,  $m \in \mathbb{N}$ , with high degree polynomials offers a fresh alternative to the use of infinitely smooth RBFs [19, 21, 22, 23, 25]. Among the key features, i) high orders of accuracy can be achieved without the need of selecting a shape parameter or the issues related to numerical ill-conditioning, ii) the edge effects associated to the use of high order polynomials (better known as Runge's phenomenon) can be easily overcome. We refer to this approach as PHS+poly approximation, and its application for the Laplace transform inversion is the core of this work. In the following, we briefly recall some definitions on RBFs and PHS essentially by following [19, 21, 22, 23].

**Definition 2.1** (PHS+poly). Given a set of (distinct) nodes  $X = \{x_i\}_{i=1}^N \subset I \subset \mathbb{R}$  and a continuous target function  $F : I \rightarrow \mathbb{R}$  sampled at the nodes in  $X$ , i.e.  $F_i := F(x_i)$ , a local PHS+poly interpolant to the data at a point  $x \in I$  takes the form

$$s(x) = \sum_{j \in \Xi(x)} \lambda_j \phi(|x - x_j|) + \sum_{k=1}^s \beta_k p_k(x), \quad (5)$$

with the matching conditions

$$\sum_{j \in \Xi(x)} \lambda_j p_k(x_j) = 0, \quad k = 1, \dots, s, \quad (6)$$

where  $\phi(|x - x_j|) = |x - x_j|^m$  is a PHS of degree  $m$ ,  $m$  odd, centered on  $x_j$ ,  $\{p_k(x)\}_{k=1}^s$  is a basis for the univariate polynomial space  $\Pi_l$  of total degree  $l$  with  $s = l + 1$ , and  $\Xi(x)$  is the subset formed by the indexes of the  $n$ -th closest nodes from  $X$  to the evaluation point  $x$ . Here,  $n = |\Xi(x)|$  (cardinality) is the *stencil size* and must satisfy  $s < n \ll N$ .

At each evaluation point  $x \in I$ , a different interpolant is computed by determining the  $\lambda$  and  $\beta$  coefficients through collocation, i.e. enforcing the conditions  $s(x_i) = F_i$ ,  $i \in \Xi(x)$ , leading to the linear system of equations

$$\begin{bmatrix} A & P \\ P^T & O \end{bmatrix} \begin{bmatrix} \lambda \\ \beta \end{bmatrix} = \begin{bmatrix} f \\ \mathbf{0} \end{bmatrix},$$

where  $A$  is the square matrix with elements

$$A = \phi(|x_i - x_j|), \quad i, j \in \Xi(x),$$

$P$  is the  $n \times s$  matrix whose  $k$ -th column corresponds with the  $k$ -th element of the polynomial basis evaluated on the collocation nodes,  $f = [F_1, F_2, \dots, F_n]^T$ ,  $\mathbf{0}$  is a zero vector of length  $s$  and  $O$  is a zero matrix  $s \times s$ . This linear system of equations is uniquely solvable when using PHS of degree  $m$  augmented with polynomials up to degree  $l \geq (m-1)/2$ , provided  $P$  is unisolvent on the node distribution (which is always the case in 1-D) [20].

In [21] was obtained the following closed-form expression for the  $\lambda$  and  $\beta$  coefficients.

**Theorem 2.1.** *Provided that  $A$  and  $P$  are full rank, the  $\lambda$  and  $\beta$  coefficients in the RBF interpolant (5) are equal to*

$$\lambda^T = f^T (I - D P^T) A^{-1} \tag{7}$$

and

$$\beta^T = f^T D, \tag{8}$$

where  $D$  is the  $n \times s$  matrix

$$D = A^{-1} P (P^T A^{-1} P)^{-1}.$$

Observe that the matrix  $D$  plays a key role in the approximation. The following result from [21] illustrates its meaning:

**Theorem 2.2.** *Let  $p(x) = x^\alpha$ ,  $\alpha = 0, 1, \dots, l$  be an element from the augmented polynomial basis  $\Pi_l$ . Then, the  $(\alpha + 1)$ -th column of matrix  $D = A^{-1} P (P^T A^{-1} P)^{-1}$  contains the differentiation weights approximating the operator*

$$L^{(\alpha)} = \frac{1}{\alpha!} \frac{\partial^\alpha}{\partial x^\alpha}. \tag{9}$$

This is, the action of (9) on  $p(x) = x^\alpha$  is equal to

$$\frac{1}{\alpha!} \frac{\partial^\alpha x^\alpha}{\partial x^\alpha} = 1 = [d_{1,\alpha+1} \dots d_{s,\alpha+1}] \cdot p|_{\Xi(x)},$$

where  $d_{i,j}$  are the elements of  $D$  and  $p|_{\Xi(x)}$  is  $p$  evaluated on the stencil nodes as in Definition 2.1.

From this result, it is straightforward to prove the following proposition, which will be useful to obtain the convergence rates of the approximation.

**Proposition 2.3.** *When the data to be interpolated comes from one of the augmented polynomial terms, i.e.  $F(x) = x^\alpha$ ,  $\alpha = 0, 1, \dots, l$ , the  $\lambda$  and  $\beta$  coefficients in the RBF interpolant (5) are equal to*

$$\lambda_j = 0, \quad \text{for } j = 1, \dots, n; \quad \beta_k = \begin{cases} 1, & \text{if } k = \alpha + 1 \\ 0, & \text{otherwise} \end{cases}, \quad \text{for } k = 1, \dots, s. \tag{10}$$

## 2.1 Convergence and asymptotic behavior results

**Theorem 2.4.** *Suppose  $x_1, \dots, x_n$  are distinct numbers in the interval  $[a, b]$  and  $F \in C^\infty[a, b]$ . Then, for an evaluation point  $x \in I = [a, b] \subset \mathbb{R}$ , the coefficients of the PHS interpolant (5) augmented with monomials of degree  $l$  are equal to*

$$\lambda_i = 0 + O(h^{l+1}), \quad i = 1, \dots, n,$$

and

$$\beta_k = \frac{1}{k!} F^{(k)}(x) + O(h^{l+1}), \quad k = 0, \dots, l,$$

where  $h := \max_{j \in \Xi(x)} |x_j - x|$ .

This can be proven as in [21], by expanding  $F$  in (7) and (8) as a Taylor series and applying Proposition 2.3 at each polynomial term. This result leads us to formulate the following corollary.

**Corollary 2.5.** *The local truncation error of the PHS+poly approximant is given by*

$$s(x) - F(x) = \sum_{k=l+1}^{\infty} \frac{1}{k!} F^{(k)}(x) [(P_k^T \cdot \hat{\psi}(x) - p_k(x)) - P_k^T W (P^T \hat{\psi}(x) - p(x))], \quad x \in [a, b],$$

where  $\hat{\psi}(x)$  is the RBF cardinal function without polynomial augmentation

$$\hat{\psi}(x) = A^{-1} \phi(x),$$

which can be bounded as

$$\|s - F\|_\infty \leq Ch^{l+1} \max_{\xi \in (a,b)} |F^{(l+1)}(\xi)|.$$

In [26] was found that cubic RBF interpolation on the interval  $[-1, 1]$  without polynomial augmentation has the end-conditions

$$\begin{aligned} s''(-1) &= s'(+1) - 2s'(-1) - \frac{3}{2}(s(+1) + s(-1)), \\ s''(+1) &= 2s'(+1) - s'(-1) - \frac{3}{2}(s(+1) + s(-1)). \end{aligned}$$

However, by augmenting the interpolant up to linear terms, i.e. enforcing the two constraints  $\sum \lambda_i = 0$  and  $\sum \lambda_i x_i = 0$ , changes to the natural cubic spline with end-conditions  $s''(\pm 1) = 0$ . This counterintuitive result connects with our discussion here.

Consider the same 1-D interpolation problem over  $n$  collocation points using cubic PHS augmented with polynomials of degree  $l$ . The cubic PHS expands as

$$|x - x_i|^3 = (x - x_i)^3 = x^3 - 3x^2 x_i + 3x x_i^2 - x_i^3$$

for  $x > x_i, i = 1, 2, \dots, n$ . Using the notation for monomials  $p_k(x) = x^k$ , it can be written as

$$\sum_{i=1}^n \lambda_i \phi(|x - x_i|) = \boldsymbol{\lambda}^T \cdot \boldsymbol{\phi}(x) = x^3 (\boldsymbol{\lambda}^T \cdot \mathbf{p}_0) - 3x^2 (\boldsymbol{\lambda}^T \cdot \mathbf{p}_1) + 3x (\boldsymbol{\lambda}^T \cdot \mathbf{p}_2) - (\boldsymbol{\lambda}^T \cdot \mathbf{p}_3),$$

where  $\mathbf{p}_k = p_k|_{\mathbb{R}(x)}$ . If  $x < x_i, i = 1, 2, \dots, n$ , the same expansion holds but with a change of sign. By Proposition 2.3, the first and second term of the equation above vanish, leading to a first order polynomial verifying the end conditions  $s''(\pm 1) = 0$ .

In general, for an arbitrary PHS  $|x - x_i|^m, m$  odd, the RBF term can be written as the polynomial

$$\boldsymbol{\lambda}^T \cdot \boldsymbol{\phi}(x) = \sum_{k=0}^m (\boldsymbol{\lambda}^T \cdot \mathbf{p}_k) x^{m-k}.$$

When augmented with polynomial terms of degree  $l$ , the interpolant at  $x \notin [a, b]$  becomes then the polynomial of total degree  $Q = \max(m - l - 1, l)$

$$s(x) = \sum_{k=0}^{l+1} (\boldsymbol{\lambda}^T \cdot \mathbf{p}_k) x^{(m-k)_+} + \sum_{k=0}^l \beta_k x^k,$$

where  $(\cdot)_+$  is the cutoff function defined by  $(x)_+ = x$  for  $x \geq 0, 0$  otherwise. Hence, when  $l + 1$  is higher than  $m$ , the PHS term in the interpolant vanishes.

Fitting models to approximate Lt were presented in [27] and in [28] it was defined a generalized smoothing spline based on the Lt asymptotic properties. In the present work PHS+poly model is considered.

### 3 PHS+poly based Laplace transform inversion by Gaver-Stehfest algorithm

We propose to substitute  $F$  by  $s$  in (2), considering the novel inversion formula:

$$f_s(t) := \frac{\ln(2)}{t} \sum_{i=1}^M V_i s(g_i), \quad t \in (0, +\infty). \tag{11}$$

It is clear that by using (11) we have an approximation error defined as:

$$\varepsilon_{approx}(t) := |f_F(t) - f_s(t)| = \left| \frac{\ln(2)}{t} \sum_{i=1}^M V_i (F(g_i) - s(g_i)) \right|, \tag{12}$$

with  $f_F$  and  $f_s$  as in (2) and (11), respectively. Considering the effects of the discretization error (4) and the approximation error (12), we are able to define the global error in  $(0, +\infty)$  as

$$\varepsilon_{global}(t) := |f(t) - f_s(t)| \leq \varepsilon_{discr}(t) + \varepsilon_{approx}(t). \tag{13}$$

The discretization error for a fixed  $M$  is reported in [13]. In this paper we estimate the computed  $\varepsilon_{approx}$ , which strongly depends on the fitting model  $s$ . The following result gives an upper bound for  $\varepsilon_{approx}$ .

**Theorem 3.1.** *Let  $F \in C^\infty(\sigma_0, \infty)$  be a Laplace Transform of  $f$ , with  $\sigma_0$  abscissa of convergence of  $F$ . Let be given  $\{(x_i, F_i)\}_{i=1, \dots, N}, \{x_1 < \dots < x_N\}$ , and defined  $s$  as in Definition 2.1. The approximation error in (12) at any  $t \in (0, +\infty)$ , with fixed  $M$ , is bounded as follows:*

$$\varepsilon_{approx}(t) \leq \frac{\ln(2)}{t} (W_I \cdot \varepsilon_F^I + W_O \cdot \varepsilon_F^O), \tag{14}$$

where

$$W_\xi := \sum_{i \in J_\xi} |V_i| \quad \text{and} \quad \varepsilon_F^\xi := \max_{i \in J_\xi} |F(g_i) - s(g_i)| \tag{15}$$

with  $\xi \in \{I, O\}$  and  $|\cdot|$  is used to refer the cardinality of the following Inner and Outer sets:

$$J_I := \{i \in \{1, \dots, M\}, \text{ s.t. } g_i \in [x_1, x_N]\} \tag{16}$$

$$J_O := \{i \in \{1, \dots, M\}, \text{ s.t. } g_i \notin [x_1, x_N]\} \tag{17}$$

*Proof.* From (12)

$$\begin{aligned} \varepsilon_{approx}(t) &\leq \frac{\ln(2)}{t} \sum_{i=1}^M |V_i| |F(g_i) - s(g_i)| = \\ &= \frac{\ln(2)}{t} \left\{ \sum_{i \in J_I} |V_i| |F(g_i) - s(g_i)| + \sum_{i \in J_O} |V_i| |F(g_i) - s(g_i)| \right\} \leq \\ &\leq \frac{\ln(2)}{t} \left\{ \sum_{i \in J_I} |V_i| \max_{i \in J_I} |F(g_i) - s(g_i)| + \sum_{i \in J_O} |V_i| \max_{i \in J_O} |F(g_i) - s(g_i)| \right\} \end{aligned}$$

with  $J_O$  and  $J_I$  defined as in (16)-(17). From (15) the (14) follows. □

We give some comments to the last result. The  $W_\xi$  values grows with  $M$ , according to the  $V_i$  definition in (3). The following table refers some computed  $W_\xi$ , for different  $M$  values, computed by MATLAB® using standard IEEE arithmetic:

$M$	$W_\xi$	$M$	$W_\xi$
4	1.0000e+02	18	3.4010e+11
6	2.3540e+03	20	7.7473e+12
8	5.4459e+04	22	1.7640e+14
10	1.2510e+06	24	4.0152e+15
12	2.8634e+07	26	9.1372e+16
14	6.5407e+08	28	2.0789e+18
16	1.4921e+10	30	4.7290e+19

H. Stehfest was among the first to be aware of the limits that inherent instability of Gaver formula posed on the ultimate results in a finite precision arithmetic system, as described in his work [16]. Stehfest recognized that with increasing  $M$  the number of correct significant digits of  $f_F(t)$  first increases and then, owing to the rounding errors, decreases. In [13] it has been found that the value of  $M$  at which the accuracy of the GS formula is maximal, is approximately proportional to the precision of the computing system is working with. Indeed, even if it seems reasonable that greater is  $M$ , a best accuracy is obtained, on the contrary, the Stehfest algorithm with  $M > 18$  by using standard type formats (up to long double real data type), suffer from numerical instability. The introduction of *arbitrary precision floating point arithmetic* helps to overcome this numerical approximation problem. In [18] some consideration about the relationship between the value of  $M$  and the standard arithmetic support the definition of two algorithms for the numerical inversion of Laplace transforms using multi-precision computing. In our experiments we'll use small value of  $M$ , so chosen taking into account the dependence of the GS points from  $M$  rather than the accuracy in the  $V_i$  computation, as argued in the next section, concerning the numerical results.

Moreover, when  $|J_I| \gg |J_O|$  and  $W_I > W_O$ , the fitting error outside the construction interval, can be assumed to be negligible compared to the estimate inside, which confers greater accuracy on the model. In these hypotheses the approximation error  $\varepsilon_{approx}$  is more finely bounded. Conversely, when  $|J_I| \ll |J_O|$ , the outer fitting error prevails providing an upper bound too wide. In general, the weighted sum in (14) gives a measure of the reliability of the inversion results, as it gives an upper bound to the amplification of the fitting errors in the solution. The following result concerns theoretical bounds for  $\varepsilon_F^I$  and  $\varepsilon_F^O$  under suitable hypothesis on  $F$ .

**Corollary 3.2.** *Let  $F \in C^\infty(\sigma_0, \infty)$  be a Laplace Transform of  $f$  with asymptotic behavior  $o(1/x^n)$  as  $x \rightarrow \infty$ , with any  $n \in \mathbb{N}$ . For a PHS+poly interpolant as in Definition 2.1 to  $F$ , the approximation error (14) is bounded as follows:*

$$\varepsilon_{approx}(t) \leq \frac{\ln(2)}{t} (W_I \cdot \varepsilon_F^I + W_O \cdot \varepsilon_F^O) \leq \frac{\ln(2)}{t} (W_I \cdot \mathcal{B}_I + W_O \cdot \mathcal{B}_O) \tag{18}$$

set

$$\mathcal{B}_I := Ch^{l+1} \max_{\xi \in [x_1, x_N]} |F^{(l+1)}(\xi)| \quad \text{and} \quad \mathcal{B}_O := o((g_i^{max})^Q) \tag{19}$$

with  $h := \max_{i=1, \dots, N-1} |x_{i+1} - x_i|$ ,  $g_i^{max} = \operatorname{argmax}_{g_i \notin [x_1, x_N]} |F(g_i) - s(g_i)|$  and  $Q = \max(m - l - 1, l) \in \mathbb{N}$ .

*Proof.* The first term in the sum (18) is proven in [21]. As concern the second term, if  $g_i \notin [x_1, x_N]$ , the interpolant becomes a polynomial of degree  $Q = \max(m - l - 1, l) \in \mathbb{N}$  when using  $\phi(r) = r^m$ ,  $m$  odd. Moreover, the extrapolation error diverges as  $o(x^Q)$ . For a proof of the second term see [22, 26]. □

*Remark 1.* We emphasize that  $\varepsilon_{global} \rightarrow 0$  if  $\varepsilon_{discr} \rightarrow 0$  and  $\varepsilon_{approx} \rightarrow 0$ ; moreover the theoretical convergence to zero of the  $\varepsilon_{discr} \rightarrow 0$  comes from increasing  $M$ ; nevertheless, the Gaver method for Laplace transform inversion is strongly ill-conditioned and the Stehfest algorithm, used to compute the Laplace inverse function, with  $M > 18$  by using standard precision, suffer from numerical instability, as just discussed. The formula amplifies the rounding errors on  $F$ , due to the  $V_i$  factors magnitude. These arguments suggest to use a limited value for  $M$ , in order to hope in a satisfactory result. Looking to the formula (18), fixed the reconstruction point,  $t$ , the larger  $M$ , bigger are the evaluation GS points, computed like  $g_i = i \cdot \log(2)/t$ ,  $i = 1, \dots, M$ ; in the next section we consider examples in which, fixed the collocation interval  $[a, b]$ , according to the  $t$  and the  $M$  values, the  $g_i$  may fall both inside and outside the construction interval. The bound  $\mathcal{B}_O$  really increases when some evaluation GS points, up to the bigger  $g_M$ , fall outside so that the model may diverge from the approximated value  $F(g_M)$ . Focusing on the reciprocal position of

the bigger knot with respect to the further GS evaluation point, we assume that the last GS point is *enough near* the maximum knot, e.g. if  $|g_M - x_N| < \epsilon$ , with  $\epsilon > 0$ , it is  $|s(g_M) - s(x_N)| < \epsilon |s'(x_N)| + \mathcal{O}(\epsilon^2)$ . An hypothesis on the distance between the last GS point, from the last knots help to understand the relation between  $M$  and  $N$  and to find a possible bound on the outer error. Particularly, if:

$$g_M - x_N = M \cdot \log(2)/t - x_N < \epsilon \Rightarrow M < \lfloor (\epsilon + x_N) \cdot t / \log(2) \rfloor$$

we can consider the following approximation for the absolute errors at  $x_N$  and  $g_M$ :

$$\begin{aligned} \varepsilon_F^O &= \max_{i \in J_0} |F(g_i) - s(g_i)| = |F(g_M) - s(g_M)| = F(g_M) - F(x_N) + \underbrace{F(x_N) - s(x_N)}_{y_N - y_N} + s(x_N) - s(g_M) \leq \\ &\leq |F(g_M) - F(x_N)| + |s(x_N) - s(g_M)| = |F'(x_N)|\epsilon + |s'(x_N)|\epsilon + \mathcal{O}(\epsilon^2) \end{aligned}$$

so that *the gradients of both  $F$  and  $s$  drive the accuracy of the bound*. We can deduce that, when  $\epsilon \rightarrow 0$ ,  $g_N \rightarrow x_N$  and  $\varepsilon_F^O \rightarrow 0$ . The  $M$  choice may help to control the distance  $\epsilon$  and, as a consequence, the upper bound for  $\epsilon \rightarrow 0$ . These arguments imply that the given error bounds do not predict the convergence of the method, with respect to  $M$ , but consider how the relation between  $M$  and  $N$  can help to control the approximation errors on the computed values of the Laplace transform inverse function, so giving only a way to approximate  $f_F$ . Finally, the bound in (18) grants the reliability of the modified GS, according with the admitted tolerance on  $\varepsilon_{global}$ .

## 4 Numerical results

In this section we focus on the reliability of the theoretical estimates for the fitting errors and their impact of the revised GS method. Unless otherwise specified, we adopt  $\phi(r) = r^7$  augmented with 8–th degree polynomials. All the simulations are carried out using MATLAB<sup>®</sup> R2018a.

### 4.1 Accuracy of PHS+poly fitting model

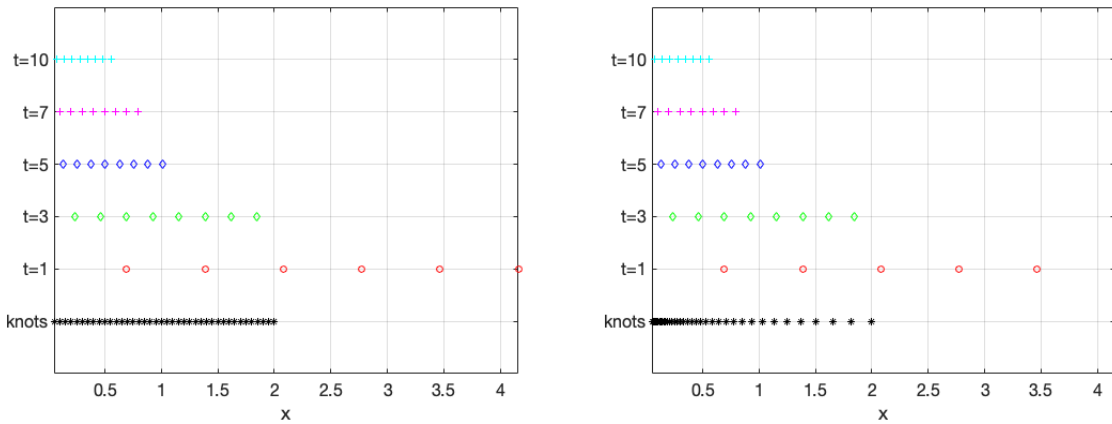
Theorem 3.1 establishes how the accuracy of the Laplace transform inversion depends on the fitting model evaluations at the GSp  $g_i = i \cdot \ln(2)/t$ ,  $i = 1, \dots, M$ , affecting the approximation error  $\varepsilon_{approx}$ . These points, which lie inside and outside the collocation interval  $[a, b]$ , depend on the number of terms  $M$  in the truncated GS formula (2). Indeed, fixed the reconstruction point,  $t$ , the larger  $M$ , bigger are the evaluation GS points values, computed like  $g_i = i \cdot \log(2)/t$ ,  $i = 1, \dots, M$ ; we consider examples in which, fixed the collocation interval  $[a, b]$ , according to the  $t$  and the  $M$  values, the  $g_i$  may fall both inside and outside the construction interval. Particularly, fixed  $t$ , increasing  $M$ , the number of the GS points falling outside increases. As concerns the  $t$  value, some basics on the Laplace transform have to be considered. As argued in the paper [13], the computation of a value  $f(t)$  requires different values of  $F$ . In GS formula the factor  $\log(2)/t$  is large when  $t$  is small, while it is small when  $t$  is large. This is a common feature of most numerical methods for inverting Laplace transforms [29], as it follows from Abelian and Tauberian theorems, which connect the behavior of the Laplace function with that of its inverse [30]. In particular, Abelian-type theorems provide information of the behavior of inverse function  $f(t)$ , as  $t \rightarrow 0$ , based on the asymptotic behavior of Laplace transform,  $F(x)$ , as  $x \rightarrow \infty$ , whereas Tauberian-type theorems provide information of the behavior of the inverse function as  $t \rightarrow \infty$ , based on the knowledge of Laplace function as  $x \rightarrow 0$ . Based on these theorems, in [13] is also proved that when  $M \rightarrow \infty$ , the asymptotic value of the global error, given by the sum of the approximation and perturbation error on the computed solution, is equal to  $f(0^+)$  (see [13] for more details and discussions). Given these arguments, in order to manage a *local* extrapolation, around the bigger collocation knot, and to control the accuracy on the computed solution, too small values for  $t$  are not recommended. This is why we use  $t = 1, 2, \dots, 10$  in our experiments.

Figure 1 describes the distribution of the evaluation points with respect to the knots interval. Particularly we represent a graph of  $N = 40$  knots uniformly (left) and geometrically (right) distributed in  $[a, b] = [0.05, 2]$ , and some GS distributions, for  $M = 6$ , and for some different  $t$ -values in  $\{1, \dots, 10\}$ , as described by the labels of the ordinate axis. In general, a fitting model can handle relatively well the approximation inside  $[a, b]$ , but will lead to large extrapolation errors outside. For instance, PHS+poly interpolants reproduce polynomials exactly up to the augmented degree  $l$  inside the collocation interval (see [21, 22]), but lead to extrapolation errors that diverge as  $o(x^Q)$ . Corollary 3.2 establishes upper bounds for both errors,  $\varepsilon_F^I$  and  $\varepsilon_F^O$ . Moreover, the accuracy of our model inside the construction interval, improves with the knots number  $N$ , as expected by the theory and confirmed by the computed results for  $\varepsilon_F^I$  in Tables 1-3. The goal of this section is to analyze numerically the effect of the truncation errors as a function of  $M$  and  $N$ .

We have considered the test function  $F(x) = 1/(x + 1)$ , whose inverse Laplace transform (iLt) is  $f(t) = e^{-t}$ , defined in the interval  $[0.05, 2]$  as in [28]. Let  $N$  be the number of equispaced collocation points in  $[0.05, 2]$  and set  $t = 1, 2, \dots, 10$  in the GS algorithm. Taking advantage of the decay behavior of the function, we do a logarithmic transformation of  $F$  and approximate  $\log F$  with PHS+poly (named as  $s_{\log}$  in the following sections). This will increase the accuracy of our PHS+poly fitting model inside the collocation interval, as it is able to reproduce polynomials exactly up to the augmented degree  $l$ , and will improve the extrapolation outside for low  $M$  values.

Tables 1-3 lists the  $\ell_\infty$  norm of  $\varepsilon_F^I$  and  $\varepsilon_F^O$  evaluated at the GSp, as a function of  $N$  and the augmented polynomial degree  $l$  for  $M = 4, 6$  and  $8$ , respectively. Observe that the approximation error inside the interval  $\varepsilon_F^I$  decreases as either  $N$  and/or  $l$  increases. The last row in each subtable shows the numerical slopes for convergence rate  $\mathcal{O}(h^{l+1})$  predicted in Corollary 3.2. Moreover, observe that  $\varepsilon_F^I$  coincides roughly for any  $M$ . This is because the GS points lie uniformly inside  $[a, b]$ .

The behavior of the approximation error outside the interval  $\varepsilon_F^O$  displays a different behavior. It saturates as  $N$  increases and does not decrease significantly as the polynomial degree  $l$  increases. As  $M$  increases, the GS points lie farther away from  $[a, b]$ .



**Figure 1:** The symbols represent the uniformly (left) and geometrically (right) distributed knots (black mark 'x') and the GS points computed for  $t = 1, 3, 5, 7, 10$ .

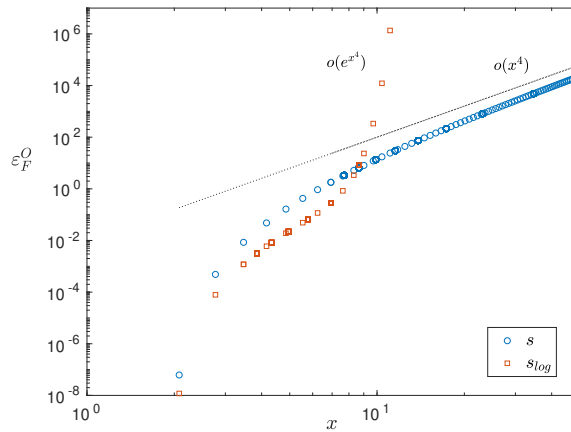


**Figure 2:**  $\ell_\infty$  norm of the error  $\varepsilon_F^O$  at the GSp for  $s$  and  $s_{\log}$  when using cubic PHS augmented with 4th degree polynomials.  $\varepsilon_F^O$  behaves as  $o(x^4)$  (black dotted line) for  $s$ , while increases as  $o(e^{x^4})$  for  $s_{\log}$ .

As stated in Corollary (3.2), the extrapolation error diverges as  $o(x^Q)$ ,  $Q = \max(m - l - 1, l)$ , and thereby, the truncation error  $\varepsilon_F^O$  increases as a function of  $M$ .

Figure 2 displays  $\varepsilon_F^O$  at the GSp for both fitting models  $s$  and  $s_{\log}$  when using cubic PHS augmented with 4th degree polynomials. Observe  $s_{\log}$  is more accurate than  $s$  for the GSp  $\lesssim 8$ . It does, however, diverge exponentially for larger GSp. This makes  $s_{\log}$  especially suited for decaying functions with low  $M$ . This logarithmic change of variable will be used in the next numerical tests, also for the compared model in [28], when it occurs.

$N$	$\varepsilon_F^l(l=2)$	$\varepsilon_F^O(l=2)$	$\varepsilon_F^l(l=4)$	$\varepsilon_F^O(l=4)$	$\varepsilon_F^l(l=6)$	$\varepsilon_F^O(l=6)$	$\varepsilon_F^l(l=8)$	$\varepsilon_F^O(l=8)$
20	1.0174e-05	9.6676e-03	2.5255e-06	2.4542e-04	3.0591e-07	6.0405e-05	4.5870e-08	2.3935e-05
40	6.5886e-06	1.3946e-02	4.7508e-07	1.1680e-04	5.0991e-08	1.3102e-05	6.0099e-09	2.0174e-06
80	3.0311e-07	2.3414e-02	2.7623e-09	7.7642e-05	4.9418e-11	5.7179e-06	3.2456e-12	5.1427e-07
160	1.2092e-08	4.1710e-02	6.2244e-11	6.2394e-05	2.6856e-13	3.6623e-06	1.8874e-15	4.8614e-06
rates	3.28	-	5.22	-	6.88	-	8.26	-

**Table 1:**  $\ell_\infty$  norm of the errors  $\varepsilon_F^l$  and  $\varepsilon_F^O$  as a function of  $N$  when using  $s_{\log}$  PHS  $r^7$  with  $l$ -th degree polynomials and stencil size  $n = l + 2$  for  $M = 4$ . The last row shows the slopes for convergence rate  $\mathcal{O}(h^{l+1})$  predicted in Corollary 3.2.

### 4.2 Comparisons between generalized spline and PHS+poly fitting models

We compare PHS+poly with the generalized smoothing spline (in the following,  $s_g$ ) defined in [28], obtained with a hybrid interpolating model, which connects, continuously, a cubic polynomial spline with a rational/exponential term acting out of

$N$	$\varepsilon_F^I(l=2)$	$\varepsilon_F^O(l=2)$	$\varepsilon_F^I(l=4)$	$\varepsilon_F^O(l=4)$	$\varepsilon_F^I(l=6)$	$\varepsilon_F^O(l=6)$	$\varepsilon_F^I(l=8)$	$\varepsilon_F^O(l=8)$
20	1.0174e-05	1.5723e-01	2.5255e-06	1.1743e-02	3.0591e-07	1.0932e-02	4.5870e-08	1.5285e-02
40	6.5886e-06	1.8232e-01	4.7508e-07	7.4676e-03	5.0991e-08	4.2502e-03	6.0099e-09	3.0987e-03
80	3.0311e-07	1.9279e-01	2.7623e-09	5.9627e-03	4.9418e-11	2.6896e-03	3.2456e-12	1.4346e-03
160	1.9531e-08	1.9799e-01	6.2244e-11	5.3262e-03	2.6856e-13	2.1405e-03	1.8874e-15	1.5985e-03
rates	3.08	-	5.22	-	6.88	-	8.26	-

Table 2: Same as Table 1 but for  $M = 6$ .

$N$	$\varepsilon_F^I(l=2)$	$\varepsilon_F^O(l=2)$	$\varepsilon_F^I(l=4)$	$\varepsilon_F^O(l=4)$	$\varepsilon_F^I(l=6)$	$\varepsilon_F^O(l=6)$	$\varepsilon_F^I(l=8)$	$\varepsilon_F^O(l=8)$
20	1.0174e-05	1.6954e-01	2.5255e-06	9.1895e-02	3.0591e-07	2.5095e-01	4.5870e-08	2.5612e+00
40	6.5886e-06	1.8232e-01	4.7508e-07	5.9709e-02	5.0991e-08	8.8790e-02	6.0099e-09	1.8298e-01
80	3.0311e-07	1.9279e-01	2.7623e-09	4.8871e-02	4.9418e-11	5.7797e-02	3.2456e-12	1.3289e-02
160	1.9531e-08	1.9799e-01	6.2244e-11	4.4341e-02	2.6856e-13	4.8318e-02	1.8874e-15	7.2358e-03
rates	3.08	-	5.22	-	6.88	-	8.26	-

Table 3: Same as Table 1 but for  $M = 8$ .

knots. Particularly, this last model consists in a *complete* cubic spline defined on  $[x_1, x_N]$ , linked with continuity up to the first order in  $x_N$  to a so-called *end behavior model*, assumed to be chosen rational or exponential. For our aims,  $s_g$  is forced to be *interpolating*. The following test compare the accuracy of the two fitting models in the approximation of two Lts with a rational and an exponential decay, respectively.

Table 4 shows the  $\ell_\infty$  error over 101 evaluation points uniformly distributed in the knots interval when approximating the following:

$$F_r(x) = \frac{2x}{(1+x^2)^2}, \quad \text{rational behavior Lt}$$

$$F_e(x) = \frac{e^{-x}}{(1+x)}, \quad \text{exponential behavior Lt}$$

by the two models,  $s$  and  $s_g$ , with  $N \in \{10, 20, 40, 60, 80, 100\}$ . For  $F_r$ ,  $N$  data values  $(x_i, F_r(x_i))_{i=1, \dots, N}$ , with abscissa *uniformly distributed* in  $[0.1, 14.6]$  are approximated. An attempt of *extrapolation* at  $[14.6, 20]$  is proved in the same table. For  $F_e$ ,  $N$  data values  $(x_i, F_e(x_i))_{i=1, \dots, N}$ , with abscissa *geometrically distributed* in  $[5, 20]$  are approximated. Numerical extrapolation at  $[20, 30]$  is also displayed in the same table. Following the results from the previous section, we do a logarithmic change of variable that smooths the decaying data, outside the collocation interval. This improves the accuracy of the PHS+poly approximation. However, it has little effect on the generalized smoothing splines model, which is typically built by enforcing a low polynomial reproduction inside the collocation interval. The same behavior carry over the following numerical tests.

$N$	$\ell_\infty(F_r)$				$\ell_\infty(F_e)$			
	$[0.1, 14.6]$		$[14.6, 20]$		$[5, 20]$		$[20, 30]$	
	$s_g$	$s$	$(s_g)_{\log}$	$s_{\log}$	$s_g$	$s$	$(s_g)_{\log}$	$s_{\log}$
10	4.2e-01	3.2e-01	2.1e-05	1.8e-04	1.3e-06	6.0e-05	3.6e-12	5.4e-14
20	1.5e-01	3.2e-02	1.7e-05	1.5e-06	2.7e-07	8.e-09	2.3e-12	3.0e-16
40	3.1e-02	1.2e-02	1.6e-05	1.1e-07	7.9e-08	2.1e-11	1.7e-12	1.7e-17
60	9.4e-03	7.9e-04	1.6e-05	5.7e-07	2.9e-08	4.2e-13	1.5e-12	9.7e-17
80	2.4e-03	1.8e-04	1.5e-05	2.5e-07	8.4e-09	1.4e-14	1.4e-12	7.1e-16
100	5.4e-05	1.5e-06	1.5e-05	4.3e-07	2.1e-10	2.3e-16	1.4e-12	3.9e-15

Table 4: Maximum accuracy for the two models,  $s$  and  $s_g$ , as a function of  $N$ .  $\ell_\infty$  norm of the error for  $F_r$  computed at 101 points, uniformly distributed in  $[0.1, 14.6]$  and  $[14.6, 20]$ .  $\ell_\infty$  norm of the error for  $F_e$  computed at 101 points, uniformly distributed in  $[5, 20]$  and  $[20, 30]$ .

### 4.3 Gaver-Stehfest inversion using PHS+poly interpolation

We use the PHS+poly model to compute the inverse Lt by the GS method. According to the definition (13), the accuracy of the solution depends both on  $\varepsilon_{discr}$  and  $\varepsilon_{approx}$ . In this section we are interested in estimating only the effects of  $\varepsilon_{approx}$ , on the computed solution; so we compare, assumed the same  $\varepsilon_{discr}$ , i.e. for fixed  $M$  and  $t$ , the results produced by our model, with those ones in [28]. To assess the accuracy of this approach, we replicate several numerical experiments as in the Section 6.2 of [28], and for this reason the distributions of nodes and evaluation points are both uniform. The test functions considered are

- (a)  $F_1(x) = 1/(x+1)$ ,  $f_1(t) = e^{-t}$ ,
- (b)  $F_2(x) = 1/(x+1)^2$ ,  $f_2(t) = te^{-t}$ ,
- (c)  $F_3(x) = 1/x^4$ ,  $f_3(t) = t^3/6$ ,

which are collocated over a uniform data distribution on the interval  $[a, b] = [0.05, 2]$  using  $N = 10, 20, 40, \dots, 120$  points. The results obtained, together with the ones computed by  $s_g$  in [28], are listed in Table 5. The accuracy is measured by means of the root mean square error of prediction (RMSEP),

$$RMSEP = \sqrt{\frac{\sum_{i=1}^P \left( \frac{s(w_i) - F(w_i)}{F(w_i)} \right)^2}{P}}, \quad P = 101,$$

where  $s$  is the interpolating model and  $w_i, i = 1, \dots, P$ , are the evaluation points, uniformly distributed in a subinterval  $[c, d]$ , such that  $[a, b] \cap [c, d] \neq \emptyset$ ; indeed, in the experiments, only the first part of the evaluation points, belonging to  $[c, d]$ , falls into  $[a, b]$ . The GS method with  $M = 4$  terms is used, and so, all the GSp fall inside  $[c, d] = [0.06931, 2.7724]$ .

Table 6 refers to the inversion results by GS. The relative errors  $|f_F(t) - f_s(t)|/|f_F(t)|$  when using the generalized spline ( $s_g$ ) and PHS+poly ( $s$ ) are listed for  $F_k, k = 1, 2$ , with  $M = 4$  terms and  $N = 40$ , and for  $F_3$  with  $M = 6$  and  $N = 120$ . Observe that the improvement in the accuracy of the fitting model, reflects on the solution of the inversion problem by several orders of magnitude.

$N$	$F_1$		$F_2$		$F_3$	
	$(s_g)_{\log}$	$s_{\log}$	$(s_g)_{\log}$	$s_{\log}$	$(s_g)_{\log}$	$s_{\log}$
10	4.2552e-03	8.1892e-04	8.4609e-03	1.6405e-03	2.7615e-01	1.3020e+03
20	3.5542e-03	9.3275e-06	7.0728e-03	1.8655e-05	1.1533e-01	1.2274e-02
40	3.2493e-03	9.0385e-07	6.4685e-03	1.8098e-06	9.0947e-02	1.2704e-03
60	3.1533e-03	4.0876e-07	6.2780e-03	7.8456e-07	8.7295e-02	2.1251e-04
80	3.1063e-03	3.6760e-07	6.1847e-03	7.0787e-07	8.5705e-02	4.9687e-05
100	3.0783e-03	5.8098e-07	6.1294e-03	1.5094e-06	8.4810e-02	3.1806e-05
120	3.0598e-03	1.1357e-06	6.0927e-03	2.6750e-06	8.4224e-02	2.5326e-05

**Table 5:** RMSEP for the two fitting models, the smoothing spline  $(s_g)_{\log}$  and the PHS+poly fitting model  $s_{\log}$ , at 101 points, uniformly distributed in  $[c, d] = [0.06931, 2.7724]$ .

$t$	$F_1$		$F_2$		$F_3$	
	$(s_g)_{\log}$	$s_{\log}$	$(s_g)_{\log}$	$s_{\log}$	$(s_g)_{\log}$	$s_{\log}$
1	1.5562e-01	7.5449e-05	8.0401e-02	3.9721e-05	1.6205e+00	9.3573e-02
2	4.7018e-08	1.3832e-12	3.7207e-08	8.0955e-13	5.8907e-03	1.3828e-10
3	6.6009e-06	1.1489e-10	5.2813e-06	7.7686e-11	1.3646e-07	3.3738e-09
4	4.8255e-05	3.2069e-10	3.4046e-05	1.9068e-10	2.0377e-05	2.3292e-07
5	1.8326e-04	8.3976e-10	1.1139e-04	4.4062e-10	3.2541e-05	4.3053e-06
6	1.3491e-04	2.7054e-10	9.0440e-05	1.3436e-10	1.9508e-06	8.1395e-08
7	3.2166e-05	4.7229e-10	1.2590e-05	2.0762e-10	6.1918e-05	6.3132e-07
8	7.0610e-04	7.2953e-10	2.3395e-04	2.8944e-10	3.8218e-03	3.1256e-05
9	1.1572e-03	3.0972e-09	5.2935e-04	6.4792e-10	1.0902e-02	8.3726e-05
10	1.9024e-02	3.1069e-08	5.0321e-03	8.1781e-09	1.1866e-02	1.0960e-04

**Table 6:** Relative error  $|f_F(t) - f_s(t)|/|f_F(t)|$  when using smoothing spline  $(s_g)_{\log}$  and PHS+poly  $s_{\log}$  for the Laplace transform inversion by GS.  $M = 4$  terms and  $N = 40$  are used for  $F_1$  and  $F_2$ ,  $M = 6$  and  $N = 120$  for  $F_3$ .

## 5 Conclusions

The numerical inversion of the Lt is an ill-posed problem. Modifying a method to compute the iLt function requires a study of several sources of error and their propagation in the inversion formula. Numerical regularization techniques are generally adopted to deal with instabilities of the numerical algorithms. In this paper, we revised the Gaver-Stehfest inversion method by introducing a powerful approximation model, the PHS+poly, to accurately fit samples of the Lt used in the GS inversion formula. For this modification, we have proved theoretical bounds on the accuracy of the fitting model. Moreover, numerical evidences of the effectiveness of the proposed scheme in the inversion problem have been presented.

## Acknowledgement

Italian authors are members of the INdAM Research group GNCS. Special thanks to the Research ITalian network on Approximation (RITA) group fostering collaboration and progress in research.

## References

- [1] D. P. Gaver, Observing Stochastic Processes, and Approximate Transform Inversion, Operations Research 14 (1966) 444–459.
- [2] P. P. Valkó, J. Abate, Comparison of sequence accelerators for the gaver method of numerical laplace transform inversion, Computers & Mathematics with Applications 48 (3-4) (2004) 629–636.

- [3] G. Doetsch, *Introduction to the Theory and Application of the Laplace Transformation*, Springer Science & Business Media, 2012.
- [4] R. Piessens, Gaussian quadrature formulas for the numerical integration of Bromwich's integral and the inversion of the Laplace transform, *Journal of Engineering Mathematics* 5 (1) (1971) 1–9.
- [5] W. Weeks, Numerical inversion of the Laplace transform using Laguerre functions, *Journal of ACM* 13 (1966) 419–429.
- [6] C. Cunha, F. Viloche, The Laguerre functions in the inversion of the Laplace transform, *Inverse Problems* 9 (1) (1993) 57.
- [7] A. Talbot, The accurate numerical inversion of Laplace transforms, *IMA Journal of Applied Mathematics* 23 (1) (1979) 97–120.
- [8] B. Dingfelder, J. Weideman, An improved Talbot method for numerical Laplace transform inversion, *Numerical Algorithms* 68 (1) (2015) 167–183.
- [9] L. D'Amore, R. Campagna, V. Mele, A. Murli, Relative. An ANSI C90 software package for the Real Laplace Transform Inversion, *Numerical Algorithms* 63 (1) (2013) 187–211.
- [10] L. D'Amore, R. Campagna, V. Mele, A. Murli, Algorithm 946: ReliAdiff—a C++ software package for real Laplace Transform Inversion based on Algorithmic Differentiation, *ACM Trans. Math. Softw.* 40 (4) (2014) 31:1–31:20.
- [11] L. Antonelli, S. Corsaro, Z. Marino, M. Rizzardi, Algorithm 944: Talbot suite: Parallel implementations of Talbot's method for the numerical inversion of Laplace transforms, *ACM Transactions on Mathematical Software (TOMS)* 40 (4) (2014) 1–18.
- [12] S. Cuomo, L. D'Amore, A. Murli, M. Rizzardi, Computation of the inverse Laplace Transform based on a collocation method which uses only real values, *J. Comput. Appl. Math.* 198 (1) (2007) 98–115.
- [13] L. D'Amore, V. Mele, R. Campagna, Quality assurance of Gaver's formula for multi-precision Laplace transform inversion in real case, *Inverse Problems in Science and Engineering* 26 (4) (2018) 553–580.
- [14] A. Murli, S. Cuomo, L. D'Amore, A. Galletti, Numerical regularization of a real inversion formula based on the Laplace transform's eigenfunction expansion of the inverse function, *Inverse Problems* 23 (2) (2007) 713–731.
- [15] R. Campagna, C. Conti, S. Cuomo, Computational error bounds for Laplace transform inversion based on smoothing splines, *Applied Mathematics and Computation* 383 (2020) 125376.
- [16] H. Stehfest, Algorithm 368: Numerical inversion of Laplace Transforms, *Commun. ACM* 13 (1) (1970) 47–49.
- [17] M. R. Naeeni, R. Campagna, M. Eskandari-Ghadi, A. A. Ardalani, Performance comparison of numerical inversion methods for Laplace and Hankel integral transforms in engineering problems, *Applied Mathematics and Computation* 250 (2015) 759–775.
- [18] J. Abate, P. Valkó, Multi-precision Laplace transform inversion, *International Journal for Numerical Methods in Engineering* 60 (5) (2004) 979–993.
- [19] V. Bayona, N. Flyer, B. Fornberg, G. A. Barnett, On the role of polynomials in RBF-FD approximations: II. Numerical solution of elliptic PDEs, *Journal of Computational Physics* 332 (2017) 257–273.
- [20] G. E. Fasshauer, *Meshfree Approximation Methods with MATLAB*, Interdisciplinary Mathematical Sciences - Vol. 6, World Scientific Publishers, Singapore, 2007.
- [21] V. Bayona, An insight into RBF-FD approximations augmented with polynomials, *Comput. Math. Appl.* 77 (9) (2019) 2337–2353.
- [22] N. Flyer, B. Fornberg, V. Bayona, G. Barnett, On the role of polynomials in RBF-FD approximations: I. Interpolation and accuracy, *Journal of Computational Physics* 321 (2016) 21–38.
- [23] V. Bayona, N. Flyer, B. Fornberg, On the role of polynomials in RBF-FD approximations: III. Behavior near domain boundaries, *Journal of Computational Physics* 380 (2019) 378–399.
- [24] B. Fornberg, N. Flyer, *A Primer on Radial Basis Functions with Applications to the Geosciences*, SIAM, Philadelphia, 2015.
- [25] N. Flyer, G. Barnett, L. Wicker, Enhancing finite differences with radial basis functions: experiments on the Navier–Stokes equations, *Journal of Computational Physics* 316 (2016) 39–62.
- [26] B. Fornberg, T. Driscoll, G. Wright, R. Charles, Observations on the behavior of Radial Basis Function approximations near boundaries, *Computers & Mathematics with Applications* 43 (3-5) (2002) 473–490.
- [27] R. Campagna, C. Conti, S. Cuomo, Smoothing exponential-polynomial splines for multiexponential decay data, *Dolomites Research Notes on Approximation* 12 (2019) 86–100.
- [28] L. D'Amore, R. Campagna, A. Galletti, L. Marcellino, A. Murli, A smoothing spline that approximates Laplace transform functions only known on measurements on the real axis, *Inverse Problems* 28 (2) (2012) 025007.
- [29] A. M. Cohen, *Numerical Methods for Laplace Transform Inversion*, 1st Edition, Springer Publishing Company, Incorporated, 2007.
- [30] D. Widder, *The Laplace Transform*, Princeton University Press, 1946.